

CONTROLLER DESIGN FOR A PLATFORM BASED AUTOMATED FINISHING SYSTEM

Gloria J. Wiens
Department of Mechanical Engineering
University of Florida
Gainesville, Florida

Nishant K. Jhaveri
Material Handling Process Segment
FANUC Robotics North America
Auburn Hills, Michigan

ABSTRACT

The majority of today's automated deburring tools face the problem that the machine tools or robots on which they are mounted have to change their orientation continuously so as to maintain the desired constant normal force along the surface geometry. This paper presents an integrated solution in which the normal force and tangential position of the cutter are instantaneously modified according to various operating conditions such as burr presence and part misalignment. The system consists of a back-drivable, two degree of freedom micro-manipulator that can be mounted to a robot, a machine tool or a parallel kinematic machine. The controller design is based on event-driven and process-based control methodologies. As a result, the cycle time and need for tedious programming is reduced, and the controller is very effective in yielding improved finishes on parts involving corners and complex contours.

INTRODUCTION

The majority of today's existing deburring tools face the problem that the machine tools or robots on which they are mounted, have to change their orientation continuously so as to maintain the desired constant normal force along the surface geometry. This requirement essentially eliminates the use of parallel kinematic machine tools (PKM) without the addition of

a rotary axis between the platform and deburring tool, or a special machine configuration. Furthermore, it is required to control both the normal force so as to maintain the consistent chamfer depth and to control the tangential position of the spindle along the feed direction. In reviewing the extensive literature in the automated finishing area and the state-of-the-art in industry, there does not exist an integrated solution to the automated chamfering and deburring problem that minimizes, if not eliminates, the above orientation issue while simultaneously responding to operating condition variations (e.g., part misalignment, burr presence).

In response to these needs, this paper presents the hybrid controller development of a back-drivable, two degree of freedom micro-manipulator that can be mounted to a robot, a machine tool or a parallel kinematic machine. Different simulation case studies and robustness studies are conducted. Comparisons are made between the controller with and without the process model based control module, which is referred to as logic module.

Background

Much of the research involved in the area of automated deburring has concentrated on constant force control strategies (active or passive compliance) or hybrid position/force control strategies (Graf, 1993; Kazerooni, 1987; Roberts et al., 1992; Stouffer et al.,

1993). An adaptive fuzzy hybrid force/position control approach was proposed to solve the problem due to robot manipulator uncertainty and complex deburring process (Hsu and Fu, 1999). The control architecture consisted of an outer loop command generator, which can automatically determine the desired robot motion profile, and inner-loop adaptive fuzzy hybrid force/position controller that can achieve real-time commands. An adaptive hybrid force/position control of a flexible manipulator for automated deburring with online cutting trajectory modification was presented to show the effectiveness of flexible manipulator in comparison with rigid manipulator (Lin and Fu, 1998).

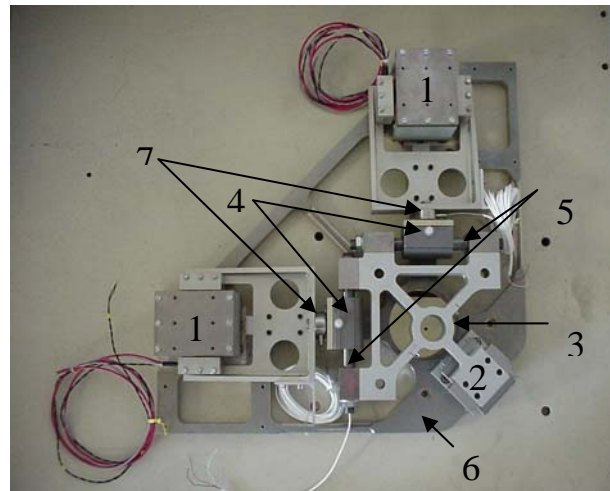
Other approaches (from the CNC perspective) for improving the performance of micro-manipulator deburring systems have integrated the XY table displacements into the control loop (Starr and Loucks, 1992). Other work has focused on the use of various types of sensor data (Starr and Loucks, 1992; Bone and Elbestawi, 1994; Dornfeld and Masaki, 1987), the development of burr minimization and removal strategies (Dornfeld and Wright, 1995), and integration of neural networks and virtual environments (Kesavadas and Khor, 1997).

PHYSICAL SYSTEM AND MODEL

Using the one degree of freedom (1-DOF), event-driven process-based controller developed by Wiens, *et al.* (1997), a major reduction in the finished edge error of approximately 84% better than that obtainable using the traditional constant force controller approach was achieved experimentally. These excellent results were obtained using an empirically derived chamfering process model rather than an 'ideal' burr model. This, superior burr removal capability of the 1-DOF micro-manipulator led to an extension of its controller and the development of a two degree of freedom (2-DOF) micro-manipulator, as presented in this paper. The impetus for adding the second degree of freedom to the micro-manipulator is for the reduction of the robot wrist movement required to maintain directional compliance and to reduce cycle time and tedious programming.

While the controller development presented in this paper is done for the 2-DOF micro-manipulator, located in the System Automation and Mobility in Manufacturing (SAMM) Laboratory, University of Florida (UF), the method should be easily applicable to 2-DOF micro-manipulators in general. The UF 2-DOF micro-manipulator is designed to be attached to the moving platform of a parallel kinematic machine (PKM), forming an automated finishing system. Figure 1 shows the 2-DOF micro-manipulator without LVDT (Linear Variable Displacement Transducer) and

spindle attached. Voice coil actuator (VCA) X and Y (#1) are angled 90° with each other. The staged, load counterbalancing slides (#2) are angled 45° degrees with respect to VCA X and VCA Y, respectively. The spindle mounting bracket (#3) is attached to VCA X and VCA Y through ball splines (#5) and ball bushings (#4). The spindle mounting bracket and ball splines – ball bushings are assembled in such a way that the force due to one VCA movement does not reflect in the other VCA direction (i.e., the movement of the VCA X does not reflect the applied VCA X force on VCA Y and vice versa). The VCA assembly base (#6) can be mounted on a robot, machine tool, or PKM. The reaction forces along the VCA X and the VCA Y axes are measured by in-line force transducers (#7).



1. TWO DEGREE OF FREEDOM MICRO-MANIPULATOR COMPONENTS (BOTTOM VIEW).

Figure 2 shows the 2-DOF micro-manipulator with coordinate frames attached to it. Frame $\{0\}$ (i.e., $\{X_0, Y_0\}$) represents the fixed inertial frame. Frame $\{\bar{1}\}$ (i.e., $\{\bar{x}_1, \bar{y}_1\}$) has the same fixed origin as the "inertial frame $\{0\}$ ". However, it's orientation remains parallel to the body affixed frame $\{1\}$, hence denoting the micro-manipulator's absolute orientation defined by 0_1R (or $R_{N(p)}$) rotation matrix. Given the position of the spindle in the $\{\bar{x}_1, \bar{y}_1\}$ coordinates corresponds to its absolute position. Frame $\{1\}$ (i.e., $\{x_1, y_1\}$) is affixed to the micro-manipulator base at the center of spindle holder travel, thus giving the relative position of the spindle (cutter) w.r.t. the micro-manipulator base (i.e., LVDT reading). The absolute position of the spindle is given by:

$$\bar{1} \begin{Bmatrix} \bar{x}_1 \\ \bar{y}_1 \\ \bar{z}_1 \end{Bmatrix} = \bar{1} \begin{Bmatrix} x_1 \\ y_1 \\ 0 \end{Bmatrix} + \begin{Bmatrix} x_3 \\ y_3 \\ z_3 \end{Bmatrix} \quad (1)$$

where $\{x_3, y_3, z_3\} = \{^1P\}$ is the displacement of the micro-manipulator's base due to robot, machine tool or PKM movement (i.e., position of the origin of frame $\{1\}$ relative to frames $\{0\}$ and $\{\bar{1}\}$). Coordinates $\{x_1, y_1\}$ are zero when the spindle is at the position that corresponds to the center of its travel. In the analysis and results, this position also corresponds to when the cutter is just touching the part's 'ideal' edge. In addition, since the micro-manipulator controller is designed relative to the micro-manipulator's base, ignoring robot, machine tool or PKM dynamics, frames $\{1\}$ and $\{\bar{1}\}$ are taken to be coincident when there is no base movement error. Also, since there is no movement of VCA in z_1 direction, the controller development is reduced to the $\{x_1, y_1\}$ directions only. Frame $\{4\}$ (i.e., $\{t, n\}$) shows the ideal tangential and normal direction of the part profile for the chamfering operation. Frame $\{5\}$ (i.e., $\{t_{act}, n_{act}\}$) shows the actual tangential and normal direction of the part profile. When the angle $\Delta\theta$ (angle between the frame $\{4\}$ and $\{5\}$) is zero, there is no part misalignment. The real-time computation of the $^4_1\bar{R}$ and 4_1R rotation matrices is not considered to be a critical issue in the controller implementation since they are a function of the nominal trajectory and can be calculated off-line a priori.

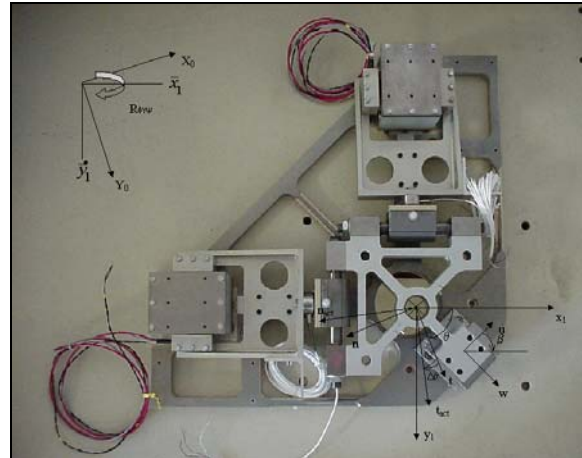
Dynamics Equation Of Motion

The dynamics of the 2-DOF micro-manipulator (ignoring z terms) is written as:

$$[M] \cdot \underline{a} = \underline{F}_{VCA} + \underline{F}_{Gravity} + \underline{F}_{friction} + \underline{F}_{reaction} \quad (2)$$

Where $[M]$ is the moving mass of the VCA/spindle assembly, \underline{a} is its acceleration, \underline{F}_{VCA} is the force applied by the VCA, $\underline{F}_{Gravity}$ is the force acting on the micro-manipulator due to gravity which depends upon the orientation of the robot, machine tool or PKM. The $\underline{F}_{friction}$ denotes the friction forces in the ball spline – ball bushing assembly and in the counterbalancing slides. The $\underline{F}_{reaction}$ represents the reaction force acting on the spindle due to chamfering and deburring operation. It is comprised of the corresponding normal (F_n) and the tangential (F_t)

force components. Additional details can be found in references Wiens et al. (1997) and Jhaveri (2000).



2. TWO DEGREE OF FREEDOM MICRO-MANIPULATOR COORDINATE SYSTEM (BOTTOM VIEW).

Reaction Forces. The load cells (#7, Figure 1) measure the forces in the VCA X and VCA Y directions that are a result of the chamfering and deburring process' normal and tangent forces. For the simulation study and the stability analysis results, these forces are calculated using the empirically derived process model used by Wiens et al. (1997). This model was obtained using a 3x3x2 designed experiment matrix for selecting test settings for the normal force, feed rate, and spindle speed. The following is the resulting process model for 45° chamfering of 4130 steel using a SGS-SA-43 STD, 1/8 in, 12 tooth, helical carbide bur, cutting at a feed rate = 8.47 mm/sec and a spindle rpm=50,000.

$$F_n(d) = \begin{cases} 0.0 & \text{if } d < 0 \\ 53.96d^3 + 2.628d^2 + d & \text{if } 0 \leq d < 0.3175 \\ -6.024d^2 + 21.94d - 4.143 & \text{if } d \geq 0.3175 \end{cases} \quad (3)$$

Where d (mm)=chamfer depth = $\bar{n}_1 - n_{2(actual)}$ and force units in N. [Note, equation (3) exhibits a small numerical error in the curve's transition at $d=0.3175$ mm. This did not create any stability issues.] The spindle normal position relative to the edge in the presence of part misalignment is

$$\bar{n}_1 = \begin{bmatrix} \cos(\theta + \Delta\theta) & \sin(\theta + \Delta\theta) \\ -\sin(\theta + \Delta\theta) & \cos(\theta + \Delta\theta) \end{bmatrix}_{row2} \begin{Bmatrix} \bar{x}_1 \\ \bar{y}_1 \end{Bmatrix} = \hat{R}_{row2} \begin{Bmatrix} \bar{x}_1 \\ \bar{y}_1 \end{Bmatrix} \quad (4)$$

The $n_{2(actual)}$ is the actual part profile with the burr. Comparing the deburring and chamfering operation to the peripheral climb milling operation, the instantaneous thrust force (F_n), is assumed related to the instantaneous cutting force (F_t) by the cutting force ratio $r = (F_n/F_t)$. This ratio is dependent on the cutting conditions. Based on the prior experimental

data analysis (Wiens et al., 1997), it is assumed to be $F_n=0.3 F_t$. These normal/thrust and tangential/cutting forces are resolved to the VCA X and VCA Y axes assuming the plane containing the normal and tangential force direction is parallel to the VCA X and VCA Y axis direction. For the simulation study, the reaction forces in the VCA X and VCA Y direction are expressed as a function of the angle between the micro-manipulator frame $\{x_1, y_1\}$ and $\{t, n\}$ of the edge to be chamfered, plus any part misalignment. That is, based on the actual tangential and the normal force direction, the reaction force ($\underline{E}_{\text{reaction}}$) is determined as

$$\begin{Bmatrix} F_{rx} \\ F_{ry} \end{Bmatrix} = \begin{bmatrix} \cos(\theta + \Delta\theta) & -\sin(\theta + \Delta\theta) \\ \sin(\theta + \Delta\theta) & \cos(\theta + \Delta\theta) \end{bmatrix} \begin{Bmatrix} F_t \\ F_n \end{Bmatrix} \quad (5)$$

Where θ is the angle between the $\{x_1, y_1\}$ frame and the ideal frame $\{t, n\}$ of the edge to be chamfered and $\Delta\theta$ is the angle between the actual tangent and normal force directions with the ideal tangent and normal force directions, respectively.

EVENT-DRIVEN PROCESS-BASED HYBRID CONTROLLER

The event-driven process-based hybrid controller is an enhanced hybrid controller for a two degree of freedom micro-manipulator. The hybrid controller's main objective is to control the tangential position by keeping the spindle (relative) position at the center of the VCA stroke and thus aligned with the micro-manipulator nominal feed and to control the normal force required to maintain the desired chamfer depth. Figure 3 illustrates the event-driven process-based hybrid controller. The sensor feedback (LVDT and force transducers) provides both force and position feedback in the X and Y directions of the micro-manipulator. In real-time, the controller resolves these values into normal force and tangential position feedback signals using rotation transformation matrix (${}^4\bar{R}$), which is evaluated using the given nominal position and orientation. Further coupling between in the position and force controllers occurs due to the fact that normal and tangential controller commands are both dependent on the resulting VCA X and VCA Y command input signals to the Deburring Head. That is, the ${}^4\bar{R}$ transforms the controller commands into resultant VCA input signals.

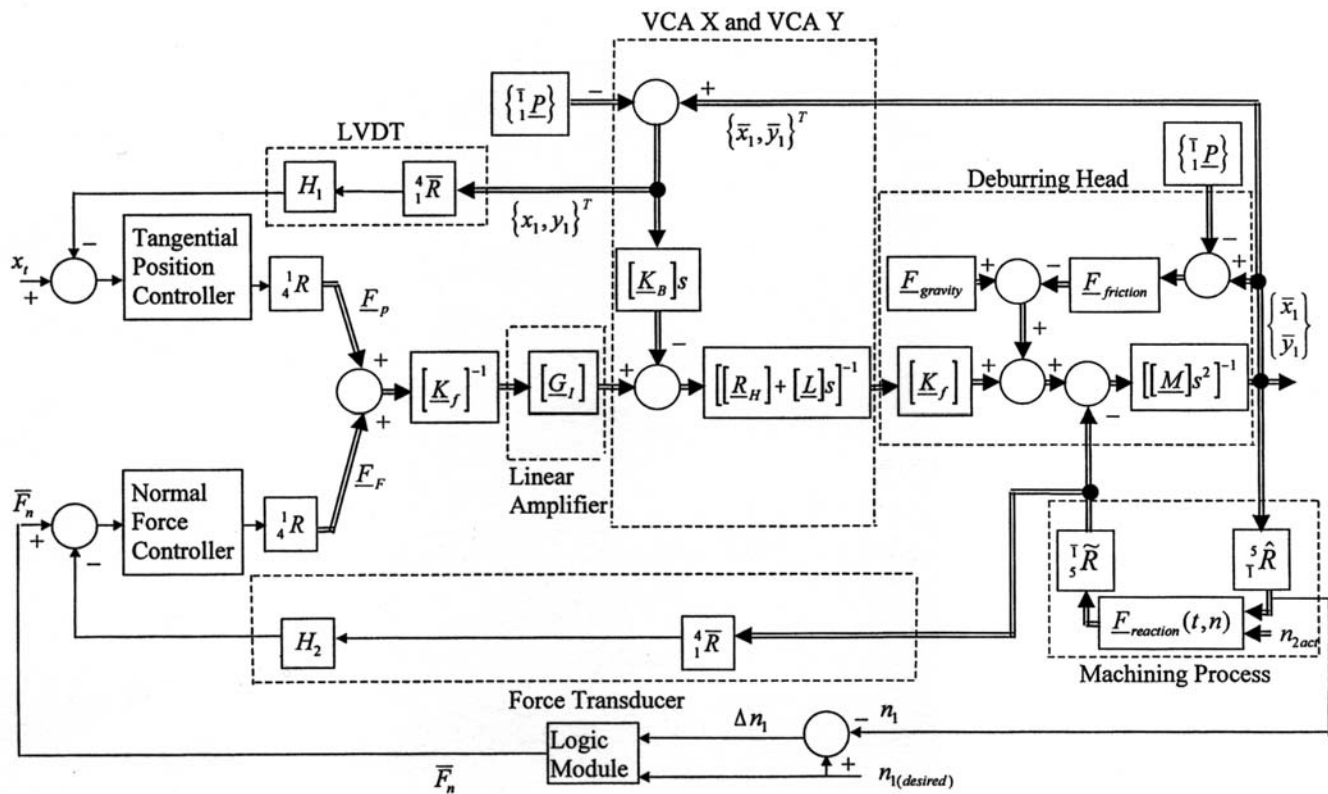
The logic module of Figure 3 uses the measured x_1 and y_1 data resolved into n_1 direction to determine the modified $d = n_1 - n_{1(\text{desired})}$. This yields $\bar{F}_n = F_n(d)$ using the process model defined by equation (3). This force value is used for modifying the normal force command value subject to the outcome of

event-driven feedback signals which trigger various reaction scenarios, e.g., burr present increase reference force \bar{F}_n , no burr no change, exit burr decrease force. That is, so as to not leave a replicate of the original unfinished edge, the constant force signal \bar{F}_n is adjusted to remove additional material in the presence of a burr. The process model is used for determining 'how much' to adjust the normal force based on the resolved normal position feedback and which event is triggered. The event triggered is based on LVDT feedback signals and knowledge of the desired edge. In the 2-DOF system, the tangential position control is coupled to the force control and simultaneously drives the relative tangent tool position to zero. The remaining terms in the block diagram of the hybrid controller are amplifier and controller gains, VCA parameters and the dynamics models of the deburring head and machining process (refer to equations 1 through 5, and Jhaveri (2000)).

RESULTS AND DISCUSSION

A modular approach was taken in the development of the hybrid controller for complex contour chamfering and deburring tasks. Both the hybrid controller scheme operating under constant force control in the normal direction and the event-driven process-based hybrid controller were tested in simulation under various operating conditions (e.g., gradual, sharp and step burrs; varying part contours including circular and pocket profiles; part misalignment and base movement errors; and noise in force feedback signal). These results demonstrated that the controller is very effective in rotating the applied normal force vector along part contours, thus eliminating the need for robot wrist rotations in maintaining the desired normal force and minimizing following errors.

Figure 4 shows the selected pocket contour (path P) using an ~50 mm square nominal trajectory to complete the task at a feedrate of 20mm/sec. In addition to the presence of burrs that can be seen by the n_{act} normal trajectory (bottom curve) in Figure 5, errors in the nominal path were introduced (~1mm base movement error). The n_d trajectory denotes the desired chamfered edge, and the n_m trajectory denotes the resulting chamfered edge. In the middle set of curves, the t_m and t_d tangential trajectories are the actual and desired positions of the spindle, respectively. The top set of curves depicts the controller effort in maintaining constant normal force and tangential position (F_{nm} and F_n are the measured and desired normal forces; and F_{tm} and F_t are the measured and desired tangential forces, respectively). Each of these plots are segmented by



3. EVENT-DRIVEN PROCESS-BASED HYBRID CONTROLLER WITH NO PART MISALIGNMENT.

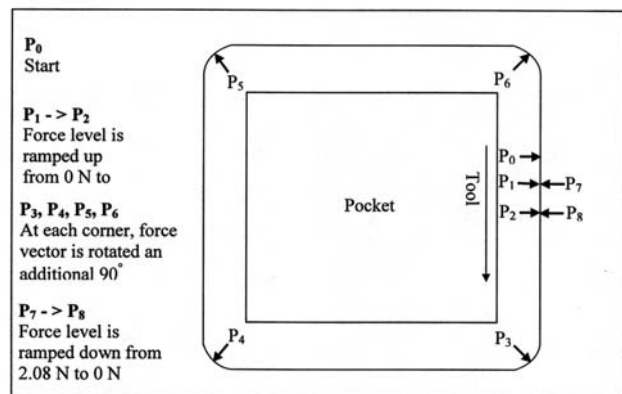
the pocket trajectory segments P_i , for $i=1,8$. The ramping of the force level, ($P_1 \rightarrow P_2$) was done to emulate the gradual engagement of the deburring head cutter with the part. This approach minimizes depressions generated due to momentary trajectory delays in switching from normal to tangential feeds. As a simplifying programming assumption, the nominal change in material removal rate in the corners was not included. However, the command force level effects due to this change can be easily accommodated in the nominal force trajectory since the nominal trajectory is known a priori. Figure 6 shows results for the same tasks and conditions, demonstrating that the logic module significantly reduced the 'replicate' of the original edge effect. The first obvious difference between Figures 5 and 6 is the significant reduction in finished edge errors (i.e., deviation of n_m from n_d); hence, minimizing the replication of the original edge (n_{act}) syndrome found in using today's industrial deburring devices.

Comparison of Hybrid Controller with and without 'Logic Module'

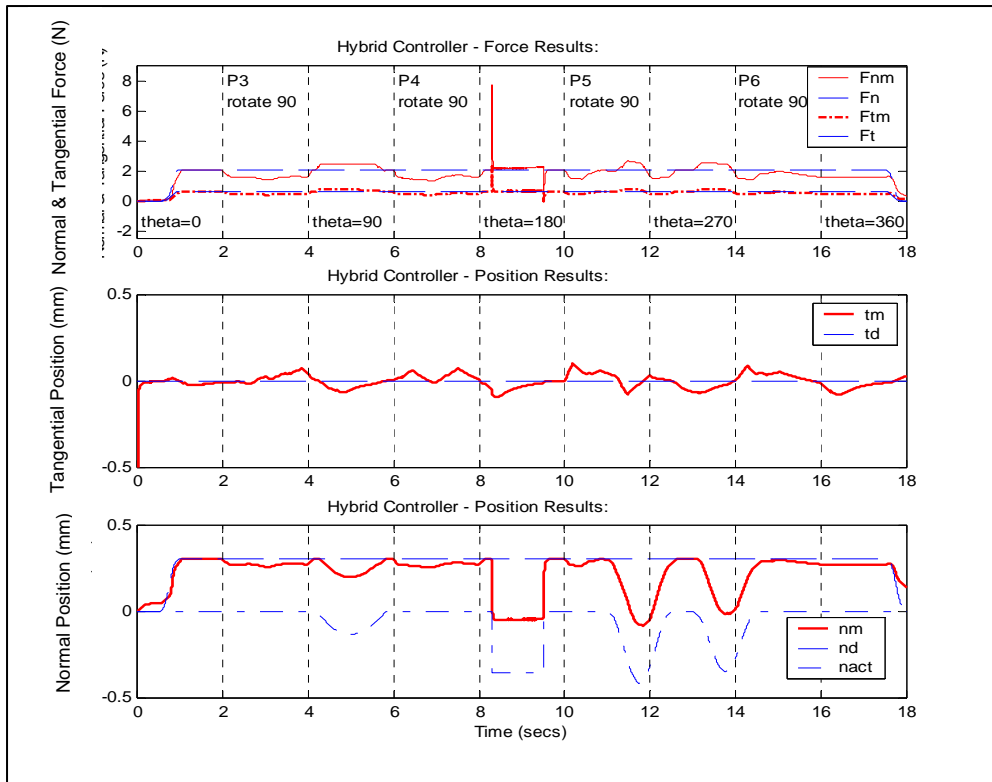
In this section, an attempt is made to demonstrate the effectiveness of process-based hybrid controller compared to the constant PI and PD based hybrid controller. The analysis is done for the case of $\theta = 0^\circ$

where the VCA X and VCA Y axes are aligned with the tangent and normal to the edge to be chamfered, respectively. That is, the hybrid-controlled system acts as a totally decoupled system in position and force control. For the case of $\theta = 45^\circ$, the hybrid-controlled system acts as coupled system. In both the cases, the friction and gravity are neglected as well as it is assumed that there is no base movement error and there is no part misalignment.

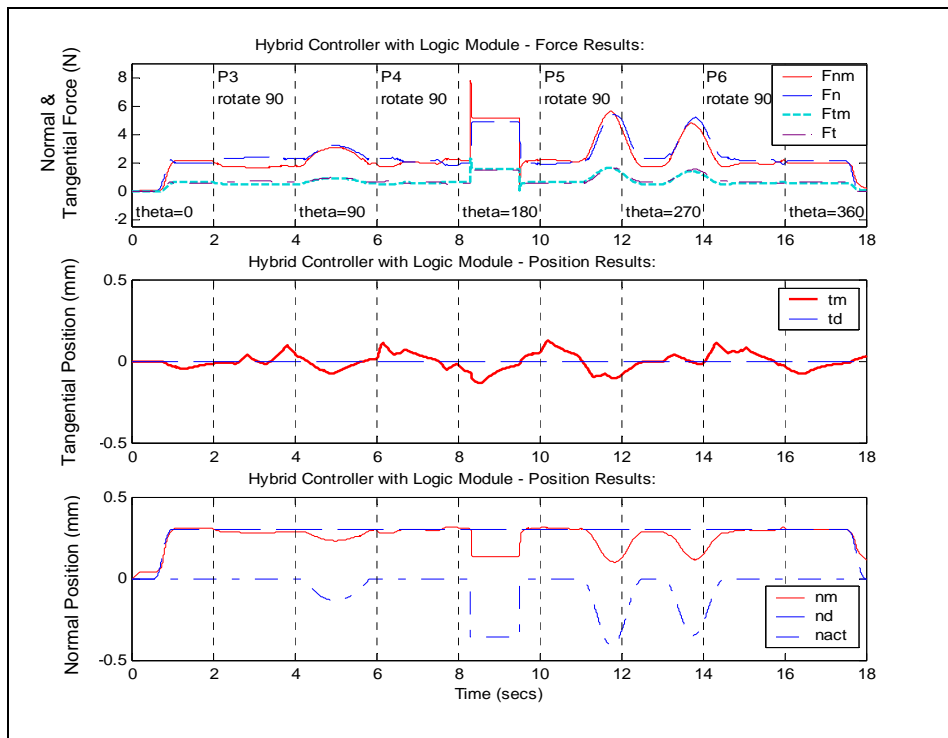
For $\theta = 0^\circ$, it was found that in the case of constant PD and PI based hybrid control, a uniform chamfer



4. CHAMFERING AND DEBURRING OF A POCKET.



5. HYBRID CONTROLLER: NORMAL FORCE, NORMAL AND TANGENTIAL POSITION. POCKET PROCESSING WITH BASE MOVEMENT ERROR.



6. HYBRID CONTROLLER WITH LOGIC MODULE: NORMAL FORCE, NORMAL AND TANGENTIAL POSITION. POCKET PROCESSING WITH BASE MOVEMENT ERROR.

depth of 0.301 mm was produced until a gradual burr was encountered. When the gradual burr occurs, the chamfer depth is initially reduced according to the burr and reaches to the lowest depth of 0.17 mm and upon exiting the burr returns to the constant chamfer depth of 0.301 mm. During the step burr, the chamfer depth is reduced to -0.004 mm from 0.301 mm and then again it returned to 0.301 mm as the burr was exited. For event-driven process-based hybrid control, the force plots indicate that the input reference force was modified when the burr was encountered. The measured chamfer depth changed from 0.303 mm to the lowest of 0.236 mm during the gradual burr and then returned back to the constant chamfer depth of 0.303 mm. The chamfer depth is changed from 0.303 mm before encountering the step burr to 0.122 mm during step burr, thus resulting in a more uniform edge.

Tables 1 and 2 give a brief summary of the resulting normal and tangential position errors for the two controllers. Although there is still error in the chamfer depth (normal position), it can be seen from Table 1 that using event-driven process-based hybrid controller with the 'Logic Module' results in a major reduction in the finished edge error by approximately 58% better than constant force, hybrid control.

In Table 2, the error in the tangential position is presented in terms of the maximum lag / lead of the spindle relative to the micro-manipulator's nominal feed. For each burr region, the spindle's maximum lag occurs when the burr is first encountered and a maximum lead occurs when exiting out of the burr. In the error responses, it is seen that the gradual burr occurs and is exited before the spindle reaches to steady state position. The settling time for the spindle tangential position during a step burr is about 1.5 seconds for the controller without the logic module and 2.0 seconds with the logic module.

While Table 2 indicates that the performance of the event-driven process-based hybrid controller is inferior to the PI and PD based hybrid position and constant force controller in terms of tangential performance, the benefits found in the normal direction (Table 1) out weigh the resulting degradation in tangential position control. The above lose of performance can be attributed to the coupling effects between the normal and tangential directions and the relative sensitivity to changes in the reference force. It should be further noted that when there are no event triggering conditions (i.e., no burrs), the two controllers become one in the same. I.e., the logic module generates no changes in the commanded input force.

Performing the same error analysis for $\theta = 45^\circ$ yielded the same normal force and tangential position errors as for $\theta = 0^\circ$; thus demonstrating the same level of effectiveness of the hybrid controller when it acts as a coupled system. Hence, it can be concluded that the hybrid-controlled 2-DOF micro-manipulator gives the same results regardless of its orientation with respect to the edge's normal and tangent to be chamfered.

Burr Region	Hybrid Controller	Event-Driven Hybrid Controller
Before step / gradual burr	1 %	0.6%
During gradual burr	13%	7.0%
During step burr	118%	60%

TABLE 1. NORMAL POSITION ERROR (AVERAGE PERCENTAGE ERROR).

Burr Region		Hybrid Controller	Event-Driven Hybrid Controller
During gradual burr	Max. lead	0.001 mm	0.018 mm
	Max. lag	0.006 mm	0.020 mm
During Step burr	Max. lead	0.041 mm	0.098 mm
	Max. lag	0.059 mm	0.103 mm

TABLE 2. TANGENTIAL POSITION ERROR.

CONCLUSIONS

To summarize, a hybrid control approach has been presented for solving the problem of excessive wrist orientation motion, tedious path programming and long cycle time during complex deburring and chamfering operation. Due to the new controller's compliance in two directions, it has been shown that the hybrid controller for the 2 DOF micro-manipulator is very effective for geometries, for which the normal to the edges varies two dimensionally in the plane of movement of the positioning device. This controller was tested for different cases like hole and square pocket processing. Its robustness was also tested under different conditions like part misalignment, base movement error and noise in the force feedback signal. This controller was modified to include the 'Logic Module' and was tested for the same cases of hole and square pocket processing. This modification enhances the controller performance by reducing the degree of replication of the original edge.

In conclusion, the simulation results of event-driven, process-based controller were impressive. Although,

there is still error in the surface, using process model based hybrid controller with event triggering correlations and logic module resulted in a major reduction in the finished edge error by about 58%. Based on the previous experience gained with the 1-DOF device (experimental results exhibited an 84% improvement over simulated results), it is anticipated that the normal and tangential errors will actually decrease further upon future implementation. One of the real advantages of this hybrid-controlled system lies in the cornering and contouring operation. This eliminates tedious orientation motion requirements in finishing complex contours as the micro-manipulator is rotating the force vector electronically around the contour. Also, the presented controllers are stable under part misalignment, base movement error and noise to a certain extent.

The future work will be the actual implementation of the presented controller in the two degree of freedom micro-manipulator system mounted on a parallel kinematic machine. Future upgrades to the controller will be advanced algorithms for distinguishing between features and burrs more accurately and for accommodating the increased material removal rate that occurs as the cutter encounters a corner.

REFERENCES

- Bone, G.M., and Elbestawi, M.A., (1994), "Sensing and Control for Automated Robotic Edge Deburring", *IEEE Transactions on Industrial Electronics*, Vol. 41, No. 2, pp. 137-146.
- Dornfeld, D.A., and Masaki, T., (1987), "Acoustic Emission Feedback for Deburring Automation," *Proceedings of Symposium on Robotic Metal Removal, ASME Winter Annual Meeting*, pp. 81-89.
- Dornfeld, D.A., and Wright, P.K., (1995), "Intelligent Machining: Global Models, Local Scripts and Validations," *Transactions of NAMRI/SME*, Volume XXIII, pp. 351-356.
- Featherstone, R., Thiebaut, S.S., and Khtaib, O., (1999), "A General Contact Model for Dynamically-Decoupled Force/Motion Control," *Proceedings of the 1999 IEEE International Conference on Robotics and Automation*, Vol. 2, pp. 3281-3286.
- Graf, T.L., (1993), "Deburring, Finishing, and Grinding using Robots and Fixed Automation: Methods and Applications," *Surface Conditioning Technical Papers*, 3M Abrasive Systems Division, St. Paul, Minnesota.
- Hsu, F-Y., and Fu, L-C., (1999), "A New Adaptive Fuzzy Hybrid Force/Position Control for Intelligent Robot Deburring," *Proceedings of IEEE International Conference on Robotics & Automation*, Vol. 3, pp. 2476-2481.
- Jhaveri, N., (2000), "Design of a Controller for a Platform-Based Automated Finishing System", Master of Science Thesis, University of Florida, Gainesville, FL.
- Kazerooni, H., (1987), "Hybrid Force/Position Control in Robotic Deburring," *ASME Winter Annual Meeting, DSC-Vol. 6*, pp. 55-63.
- Kesavadas, T., and Khor, C., (1997), "A Neural Network Based Interactive Programming of a Deburring Robot in a Virtual Environment," *ASME International Mechanical Engineering Congress and Exposition, MED-Vol. 1*, 273-280.
- Lin, I-C., and Fu, L-C., (1998), "Adaptive Hybrid Force/Position Control of a Flexible Manipulator for Automated Deburring with On-Line Cutting Trajectory Modification," *Proceedings of IEEE International Conference on Robotics & Automation*, Vol. 1, pp. 818-825.
- Roberts, R.K., Engel, T.W., and Proctor, F.M., (1992), "Specification of an Active Force Control Tool for Performing Deburring and Chamfering on a Robot Platform," *Proceedings of International Conference on Industrial Electronics, Control, Instrumentation and Automation (IECON)*, pp. 918-926.
- Starr, G.P., and Loucks, C.S., (1992), "Edge Finishing Using Hybrid Position/Force Control of an XY Table," *Proceedings of International Conference on Industrial Electronics, Control, Instrumentation, and Automation (IECON)*, pp. 934-939.
- Stouffer, K., Michaloski, J., Russell, B., and Proctor, F.M., (1993), "ADACS - An Automated System for Part Finishing," *Proceedings of International Conference on Industrial Electronics, Control, Instrumentation and Automation (IECON)*, pp. 581-586.
- Wiens, G.J., Musunur, L.P., and Walker, C.W., (1997) "Process Model-Based Force Controlled Chamfering and Deburring", *Journal of Vibration and Control, Special Issue on Machining and Finishing Processes*, Vol. 3, No. 3, pp. 331-350.

ACKNOWLEDGEMENTS

Funding for the 2 DOF micro-manipulator test bed has been provided in part by NSF Grants No. DMI-9800806 and DMI-9622328.